Available online at www.sciencedirect.com

ScienceDirect

Procedia Environmental Sciences 25 (2015) 206 – 213

Procedia Environmental Sciences

7th Groundwater Symposium of the
International Association for Hydro-Environment Engineering and Research (IAHR)

A spectral multidomain penalty method solver for the simulation of the velocity attenuation in hyporheic flows

J. A. Peñaloza Giraldo[a]*, J. A. Escobar-Vargas[b] and L. D. Donado[c]

[a]*Department Civil and Agricultural Engineering, National University of Colombia, Bogotá – 11001000, Colombia*
[b]*Department Civil Engineering, Pontificia Javeriana University, Bogotá – 11001000, Colombia*
[c]*Department Civil and Agricultural Engineering, National University of Colombia, Bogotá – 11001000, Colombia*

Abstract

A hydrodynamic model, based on a spectral multidomain penalty method (SMPM), is proposed to study the dissipation of the velocity fluctuations at the hyporheic zone. The model is based on the one dimensional Navier Stokes equations, assuming incompressibility and a hydrostatic approximation. The spatial discretization of the governing equations is done via the SMPM that is a multidomain collocation approach based on discontinuous non-overlapping subdomains that are connected by a penalty term that ensures stability of the solution by imposing weak continuity at the subdomain interfaces. The temporal discretization of the equations is handled with a high-order fractional time step technique. A spectral filter is used to stabilize the solution when spurious oscillations appear in the solution. A sinusoidal pulse is imposed at the water/sediment interface as a boundary condition, and the flow dynamics was evaluated under different conditions of kinematic viscosity. A progressive damping of the velocity fluctuations was observed in all cases, until full dissipation is reached. At that point, the flow can be governed by Darcy's law.

Peer-review under responsibility of the Scientific Committee of the IAHR Groundwater Symposium 2014

Keyword: hyporheic zone; hydrodynamic; velocity fluctuation; numerical model; spectral multidomain penalty method

1. Introduction

The various biochemical and physical processes in the water/sediment interaction are essential for the development of vegetation and animal survival [1]. The existence of inappropriate substances from anthropogenic activities causes the death of the biota. The interstitial spaces of the sediment particles are preferential flow paths, which also is the place for the accumulation of a wide variety of macroinvertebrates [2, 3]. This species are essential for the survival of fish in the first phase of life, such as Salmon [4, 5].

*Corresponding author. Tel: +57 1 3165000 Ext. 13475
E-mail address: joapenalozagi@unal.edu.co

Peer-review under responsibility of the Scientific Committee of the IAHR Groundwater Symposium 2014
doi:10.1016/j.proenv.2015.04.028

Hyporheic flow is the interaction between surface flux and subsurface flux i.e., water that is flowing in the stream channel flows into the subsurface materials of the streambed and then returns to the stream [6]. The scientific community is currently interested in the transport processes that happen in this type of flows [7]. Mathematical prediction is essential for resource management but some phenomena are ignored because analytical or computational limitations. When speaking of flow in porous media, the inertial forces are negligible compared to viscous forces. This assumption cannot represent the physical processes in turbulent rivers where nonlinear effects have to be taken into account. Various theories have been raised about the turbulence in the porous medium taking into account the scale of micro-and macro-turbulence [8, 9, 10]. Experimental tests have been designed to study turbulent phenomena associated with the velocity and pressure when the Reynolds number Re $\leqslant$ 1740 [11, 12, 13]. Measurements of the velocity in hyporheic zone with surface turbulent flow have evidenced how the velocity fluctuations are damped by effect of the porosity [14, 15].

To the authors's knowledge, the mathematical modeling of turbulent flows in porous media has not been explored enough to be introduced into commercial codes. The nonlinear effects of the momentum equation cause errors in numerical methods of low order as finite differences or finite elements due to the numerical diffusion [16]. To solve this problem, we have explored the possibility of using high-order element based-methods (spectral), taking into account that these methods do not present problems of numerical diffusion [27]. Stefan and Higashino [17] have used the Fourier spectral method for observing the damping of a sinusoidal pulse that represent the velocity fluctuation due to turbulent processes in the sediment. However, the method uses periodic boundary conditions, situation that restricts the physical representation of the phenomenon.

Taking into account the above situation and trying to use the advantages of the methods based on elements, this paper explores the potential of the Spectral Multidomain Penalty Method (SMPM), which through a discontinuous collocation type approach allows simulating these phenomena with no periodic boundary conditions.

2. Governing equation

The starting point was the one dimensional incompressible Navier-Stokes equation (1)

$$\frac{\partial w}{\partial t} + w\frac{\partial w}{\partial z} = -\frac{1}{\rho}\frac{\partial P}{\partial z} + \upsilon\frac{\partial^2 w}{\partial z^2} + g \qquad (1)$$

where w is the vertical component of the velocity, P is the pressure, υ is the kinematic viscosity of the water, and g is the gravitational constant. If hydrostatic flow is assumed, the pressure gradient can be represented as $\partial P/\partial z = -\rho g$. This assumption gave rise to the Burgers equation (2). From the physical point of view, the apparent kinematic viscosity υ is the parameter representing the damping capacity of the velocity w as it flows through the sediment, till reaching the point where Darcy's law applies.

$$\frac{\partial w}{\partial t} + w\frac{\partial w}{\partial z} = \upsilon\frac{\partial^2 w}{\partial z^2} \qquad (2)$$

2.1 Boundary conditions and initial

Because the goal of the present work is to include velocity fluctuations, the boundary condition at the sediment/water interface was defined as a decomposition of a mean velocity W, and a perturbation w' given as a sinusoidal pulse (see equations (3) and (4)) [17]. The boundary condition at the bottom is given by equation (5).

$$w(0,t) = W + w' \quad (3) \qquad w' = U\sin\frac{2\pi t}{T} \quad (4) \qquad w(L,t) = W \quad (5)$$

In equations (3), (4) and (5), U is a characteristic velocity (pulse amplitude), usually taken as 1 cm/s, t is the time, T the period and L the sediment depth. Figure 1 shows a schematic of the physical process being modeled in this work. The upper boundary condition has the effects of turbulent flow surface. The transient layer is affected by the nonlinearity of the velocity, hence the velocities fluctuations w' are present. When the velocities fluctuations are damped by the porous medium, the velocity behaves linearly so the Darcy law can apply. The bottom boundary condition assumes that w is constant after passing completely through the transient layer, therefore its value is equal to the average velocity. It should be noted that this does not represent the total reality, since it has demonstrated with Particle Image Velocimetry (PIV) how the velocity decreases with depth in the sediment [14, 15, 18].

The initial condition was defined as $(z, 0) = W$ i.e., the porous medium preserves the laminar flow before of starting the displacement of the disturbance.

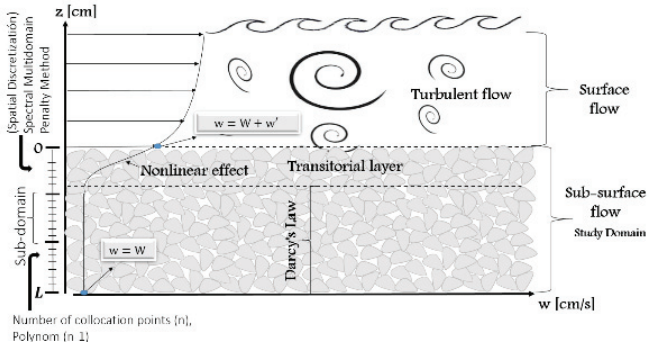

Fig. 1. Schematic velocity profile in the interaction water / sediment

2.2 *Properties of the porous medium*

As mentioned above, the apparent kinematic viscosity ν defines the damping of the velocity pulse caused by the turbulent flow processes at the sediment/water interface. Equation (6) presents the relationship between the kinematic viscosity ν, and porous media parameters [19, 20, 21, 22]. Equation (7) presents a more detailed definition of the variables used in (6) such as: grain size d, the medium porosity φ, hydraulic conductivity K and the acceleration of gravity g [23,24].

$$\nu = \frac{\varphi}{K}\, x\, \frac{g d^2}{32} \quad (6) \qquad K = \frac{5.6x10^{-3}\varphi^3 {d_s}^2}{(1-\varphi)^2} x \frac{g}{\upsilon_0} \quad (7) \qquad \upsilon = \left(\frac{\upsilon_0}{32}\right)\left(\frac{1}{5{,}6x10^{-3}}\right)\left(\frac{d}{d_s}\right)^2 \quad (8)$$

When replacing equation (7) into equation (6), we obtain equation (8), in which υ_0 is the kinematic viscosity for pure water and d_s is the sediment grain diameter. Figure 2 shows a plot of the porosity φ v.s viscosity υ for different relationship of the scale of the pores and the sediment particle diameter d/d_s. From the same figure it can be observed that there is a high viscosity when the porosity is low, i.e., the velocity slowly diffuses but is induced damping faster.

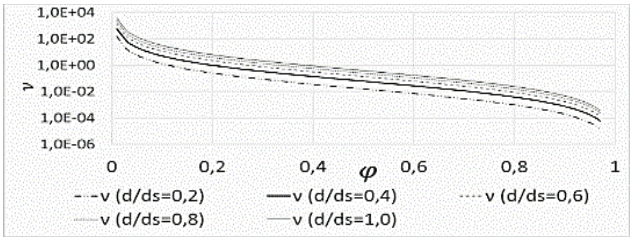

Fig. 2. Viscosity in terms of the parameters of the porous medium

3. Numerical method

3.1 Temporal discretization

In order to reduce the numerical errors introduced by the advective term, the skew-symmetric form of the nonlinear operator is used (see Equation (9))

$$\frac{\partial w}{\partial t} + \underbrace{\frac{1}{2}\left[w \cdot \frac{\partial w}{\partial z} + \frac{\partial}{\partial z}(w \cdot w)\right]}_{N(w)} = \underbrace{\upsilon \frac{\partial^2 w}{\partial z^2}}_{L(w)} \quad (9)$$

For the temporal discretization of the governing equation (9) a scheme of higher order fractional steps was used [25]. In this scheme the nonlinear term $N(w)$ was solved explicitly by a method of Adams-Bashforth third order and the viscous term $L(w)$ was solved implicitly by iterative solution GMRES due to not symmetrical matrix structure [9].

According to the scheme, if the equation (9) is integrated in time t_n to t_{n+1} the following semi-discrete equations decomposed into two fractional steps to w (10) (11) are obtained:

$$\frac{\widehat{w} - \sum_{q=0}^{J_i-1} \alpha_q w^{n-q}}{\Delta t} = \sum_{q=0}^{J_e-1} \beta_q N(w^{n-q}) \quad (10) \qquad \frac{\gamma_0 w^{n+1} - \widehat{w}}{\Delta t} = \upsilon \frac{\partial^2 w}{\partial t^2}\Big|^{n+1} \quad (11)$$

The coefficients $\alpha_q \beta_q$ in equation (10) and γ_0 in equation (11) correspond to a third order scheme rigidly stable (SS3) [25]. Their values can be found in [25, 26].

3.2 Spatial discretization

This method is based on a collocation approach applied to multiple subdomains (elements) in one dimension. In each subdomain, any function $w(z,t)$ is approximated as

$$w(z) = \sum_{i=1}^{N} \widehat{w_i} P_i(x) \quad (12)$$

where P_i are orthogonal polynomials (Jacobi (Legendre), periodic functions, etc.) that can be calculated hierarchically, $\widehat{w_i}$ are coefficients modals or modes and N is the number of modes in the approximation.

For more details on the numerical method implementation, and the specific treatment of the advective and viscous/ diffusive operator, see references [28, 29, 30, 31].

3.3 Additional stabilization strategies

Incorporation of a multidomain penalty scheme in the flow solver provides enhanced numerical stability properties that allow for simulations with higher degrees of under-resolution. However, this enhancement of numerical stability holds only in the vicinity of subdomain interfaces and physical boundaries [27]. For a higher-order polynomial discretization, additional measures need to be implemented to ensure numerical stability of the solution in the interior of a subdomain. To this end a spectral filtering [32] is applied after each fractional step (Equations (10)–(11)) in the temporal discretization. Finally, an interfacial averaging procedure [27] is applied at the subdomain interfaces. Implementation details on all three of the aforementioned procedures may be found in reference [33].

4. Setting the numerical modeling

4.1 Boundary condition and viscosity

From equations (3) and (4) were selected 2 different configurations for the boundary condition. The period T gave the characteristic velocity pulses (Figure 3). The pulses 1 and 2 had periods T in 1 s and 1.5 s respectively. Each pulse was modeled for different viscosities depending on the parameters of the porous medium (Figure 2). The Reynolds number was obtained as $Re = Ul/\nu$ where l is a characteristic length scale, which was taken to be the wave length of the pulse $l = WT$ [17], U is the characteristic velocity defined in (4), and ν is the kinematic viscosity defined by (8).

4.2 Discretization and spectral filter

For all test cases, a polynomial of degree N=15 was used, and a total 30 subdomains were used in the vertical direction. This configuration gave a total of 480 points of global positioning. The domain extent considered the first 100 cm from the water/sediment interaction. Finally simulations are performed for the first 150 s with a time interval of $5.072\text{x}10^{-3}$s, deducted by a $CFL = 0.1$

To eliminate the numerical noise produced by the nonlinear iterations well known as the Gibbs phenomenon a spectral filter was introduced [32]. Additionally, the modeling was performed with a flexible filter.

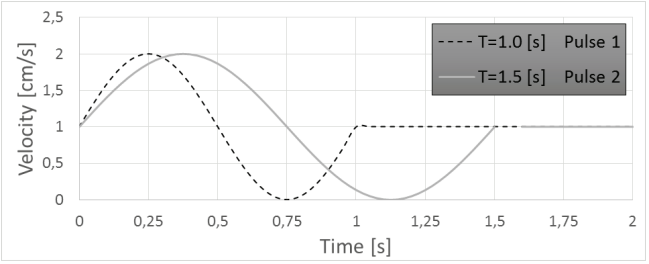

Fig. 3. Configurations of the boundary conditions at the water/sediment iteration. Amplitude U = 1 cm/s, average velocity W = 1 cm/s.

5. Numerical results

5.1 Run 1 ($T = 1.0\ s$)

Pulse 1 represented lower period. In this run numerical instabilities were seen for low viscosities ($\nu \leq 0.01$ cm^2/s, see figure 4a and 4b). This behavior was observed by unexpected additional oscillations at different depths (0.2 cm and 1 cm). In the same figures, it can be observed that due to the low viscosities, a fluctuation of the velocity is still detected. As expected, if the viscosity increases ($\nu \geq 0.3 cm^2/s$), as in figures 4c and 4d, the dissipation of the velocity occurs in a shorter period of time. After that point the flow is governed by Darcy's law.

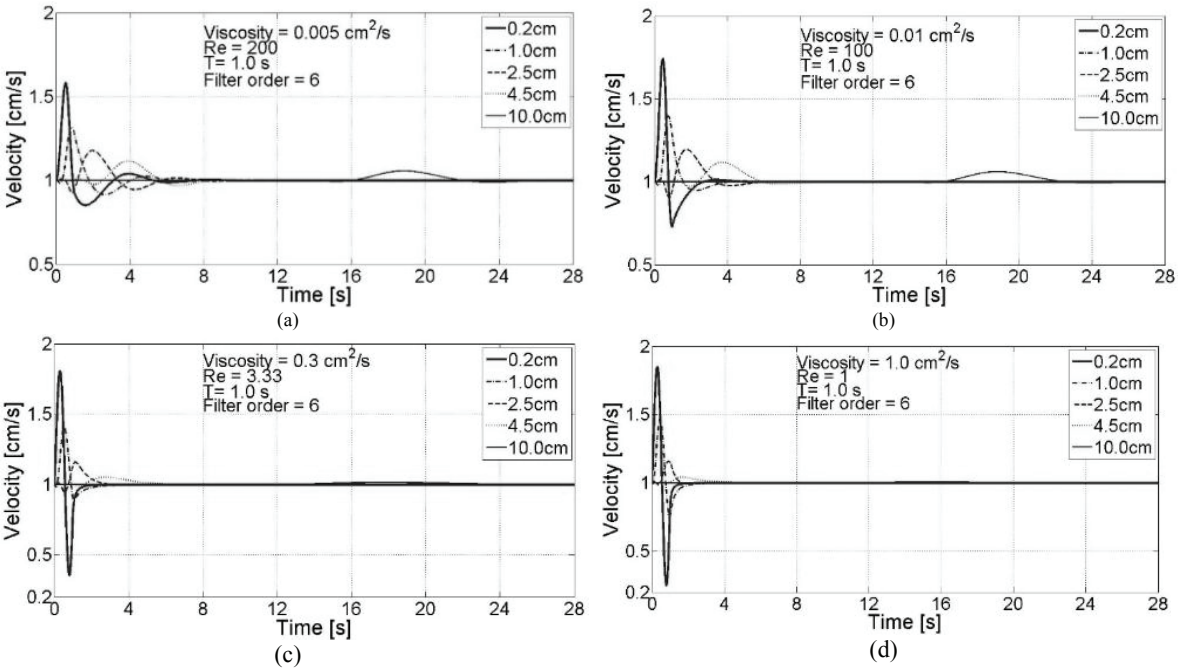

Fig. 4. Evolution of the pulse in the first 10 cm of depth in the sediment with variable viscosity and period T = 1.0 seconds.

5.2 Run 2 ($T = 1.5\ s$)

In this run, the same oscillatory behavior, as in the previous case, was observed for the lower viscosities (figures 5a and 5b). As expected, the higher the viscosity, the faster the damping of it. When compared with the previous case, it is clear that due to the higher period (*T*), the velocity fluctuation remains for a longer period of time.

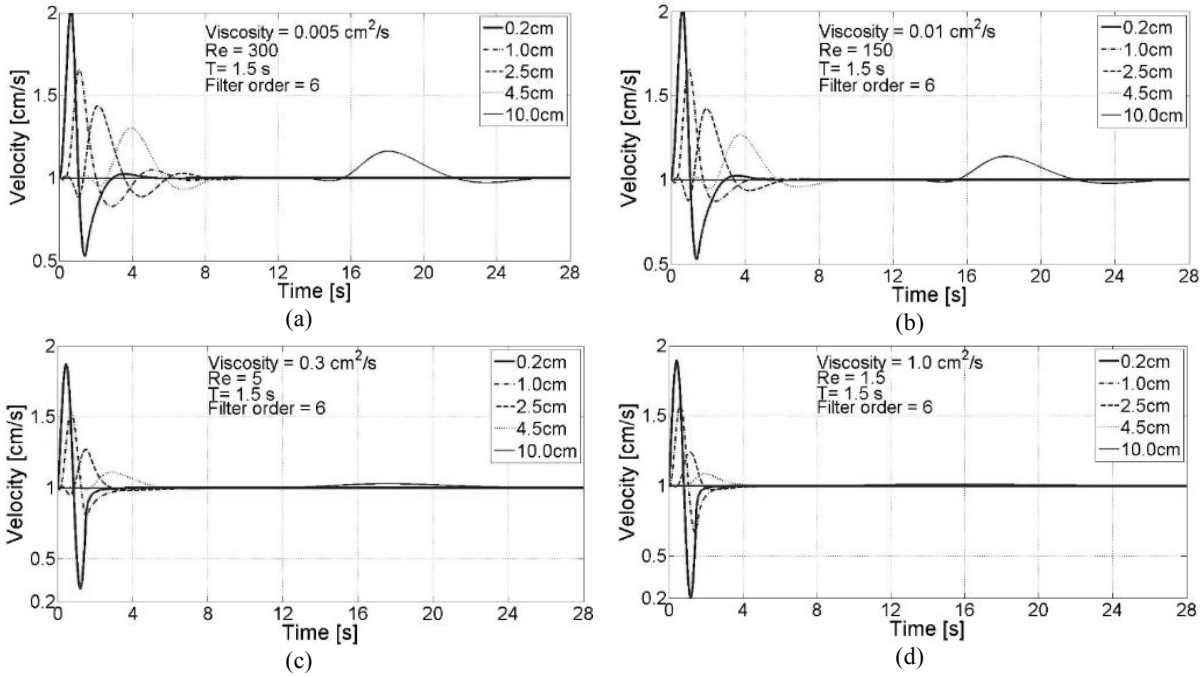

Fig. 5. Evolution of the pulse in the first 10 cm depth in the sediment with variable viscosity and period T = 1.5 seconds

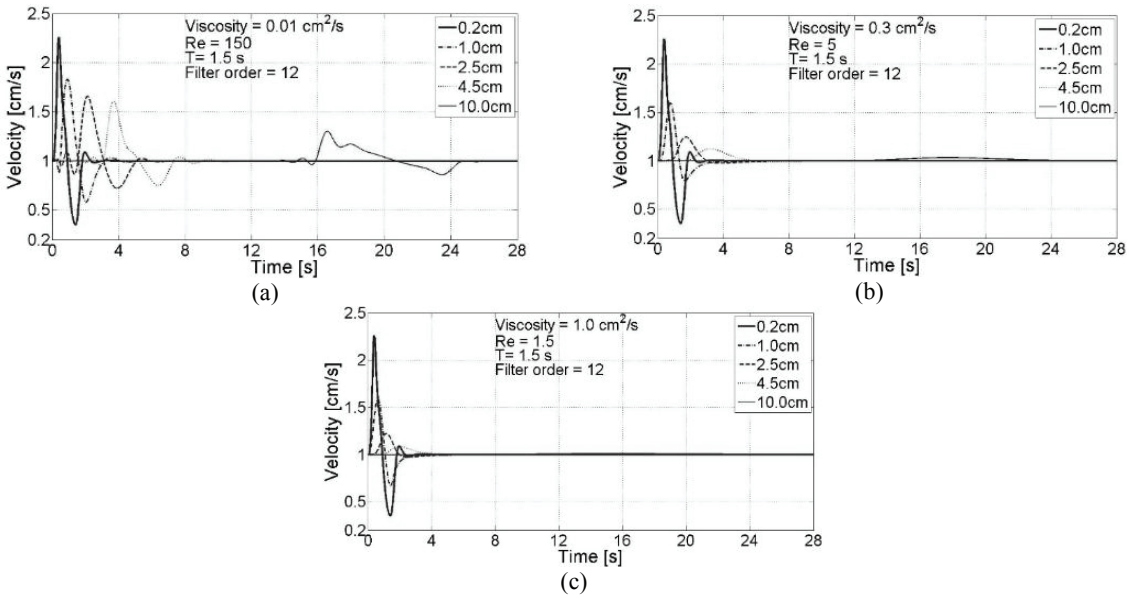

Fig. 6. Evolution of the pulse in the first 10 cm of depth in the sediment with variable viscosity, Period T = 1.5s and the order filter 12.

5.3 Spectral filter

To evaluate the effects of the spectral filter, the second pulse was used to analyze its behavior. A filter of order 12 was applied to compare the results with the existing ones with filter order 6. Note that the effect of the filter on the solution increases when the order of it decreases. For details about the mathematical basis of this filter see [32].
The first thing to note in figure 6 is that there is not a plot for $\upsilon \leq 0.005$ cm^2/s. It is attributed to the fact that the numerical instabilities dominated the simulation, making it to blow up. In figure 7a a solution with spurious oscillations can be observed, in such a way that it cannot be considered as a reliable solution. Once the viscosity increases($\upsilon \geq 0.01 cm^2/s$), the effect of the viscous forces tends to be stronger, and for that reason the solution is more stable.

6. Conclusions and future work

In this paper the damping of a velocity fluctuation inside the hyporheic zone was presented for different configurations of boundary conditions (pulse period), and viscosities. The latter being a function of the sediment porosity, where higher values of it represent lower values for the viscosity. As expected, the lower the viscosity, the higher the Reynolds number, and subsequently, the more unstable is the solution.

As mentioned in section 5.4, when the porosity is greater than 0.4 ($\upsilon = 0.005$ cm^2/s) the solution becomes unstable due to the increase in Reynolds number. To solve this problem, a more detailed analysis has to be done where the number of degrees of freedom in the domain has to be increased to capture the additional scales that appear for that Reynolds number. An alternative to deal with this problem is to make use of a spectral filter, but special attention has to be taken if the period of the velocity pulse at the boundary becomes smaller than $T \geq 1.5$ s. It was observed that the effect of the filter for $\upsilon \geq 0.3$ cm^2/s ($Re \leq 333.333$) can be negligible.

Based on figures 4 and 5 we conclude that once the pulse enter into the hyporheic zone, its structure becomes asymmetric because the negative velocity perturbations ($w' \leq 0$) are damped faster, due to the effect of viscous forces, than the positive ones. These results were different to the ones presented by Higashino and Stefan [17], where the structure of the pulse into the hyporheic zone remains symmetric. For all cases it was observed that once the velocity pulse reached the end of the transitional layer, the flow is governed by Darcy's law.

The spectral multidomain penalty method is a robust tool for modeling flows with nonlinear processes, and non-periodic boundary conditions. As expected, this technique does not present problems of numerical diffusion during hydrodynamic modelling; however, the instability caused by the non- linear advection term, when the Reynolds number becomes high, is inevitable. Future work should aim at development of spectral filters for high Reynolds numbers, taken into account that in these situations is where the biggest problems of numerical instability are presented.

Although initial and boundary conditions defined in this paper were sufficient to evaluate the damping of the velocity pulse, it is clear that the average velocity in the porous medium W varies with the depth. In this regard, the next step focuses on using the initial condition as a non-constant function that represents the decay of the average velocity$W$. In the same vein, given the flexibility offered the method to work with non-periodic boundary conditions, an imposition of the bottom boundary condition with the average velocity value given by the initial condition, i.e., ($W(L,t) = W(L,0)$) will be analyzed, where L is the maximum depth of the sediment.

Identifying the influence of turbulence in the sediment/water interface, by means of a turbulent viscosity, can help to integrate the flow dynamics with mass transfer models in the hyporheic zone. By implementing water quality models in porous media under the influence of turbulence will allow to predict more accurately the processes associated with mass transfer. In this regard, future research aims to implement a multi-rate mass transfer model in the sediment considering the heterogeneous medium that includes the effects of velocity perturbations.

References

[1] Connor, B. L., Harvey, J. W. Scaling hyporheic exchange and its influence on biogeochemical reactions in aquatic ecosystems. Water Resources Research, 2008:**44**:1029.
[2] Williams, D., Hynes, H.B.N. The occurrence of benthos deep in the substratum of a stream. Freshwater Biology, 1974:**4**:233–256.
[3] Olsen, D.A.,Townsend, C.R. Hyporheic community composition in a gravel-bed stream: influence of vertical hydrological exchange, sediment structure and physicochemistry. Freshwater Biology, 2003:**48**:1363–1378.
[4] Bjornn, T. and Reiser, D. Habitat requirements of salmonids in streams. American Fisheries Society Special Publication, 1991:**19**:83–138.
[5] Franssen, J., Lapointe, M. and Magnan, P. Geomorphic controls on fine sediment reinfiltration into salmonid spawning gravels and the implications for spawning habitat rehabilitation. Geomorphology, 2014:**211**:11-21.
[6] Bencala, K. Hyporheic Exchange Flows. United States Geological Survey, MG Anderson and McDonnell JJ., 2005:1-7.

[7] Wondzell, S. M. and Swanson, F. J. Seasonal and storm dynamics of the hyporheic zone of a 4th-order mountain stream. The North American Benthological Society, 1996:**15**:1-19.
[8] Lage, J. The fundamental theory of flow through permeable media from darcy to turbulence. Transport Phenomena in Porous Media. Derek B. Ingham and Iaon Pop, 1998:1-30.
[9] Lage, J., De Lemos, M., Nield, D. Modeling turbulence in porous media. Dalllas: Southern Methodist University, 2002.
[10] Pedras, M. H. and De Lemos, M. On the definiton of turbulent kinetic energy for flow in porous media. International communications in heat and mass transfer, 2000:**27**:211-220.
[11] Barr, D. Turbulent flow through porous media. Ground water, 2001:**39**:646-650.
[12] Masuoka, T. and Takatsu, Y. Turbulence characteristics in porous media. In Transport Phenomena in Porous Media II. Elsevier; 2002:221-256.
[13] Seguin, D., Montillet, A., Comit, J. and Huett, F. Experimental characterization of flow regimes in various porous media-II:Transition to turbulent regime. Chemical engineering science, 1998:**5**:3897-3909.
[14] Pokrajac, D., Manes, C., and McEwan, I. Peculiar mean velocity profiles within a porous bed of an open channel. Phys. Fluids, 2007:**19**.
[15] Pokrajac D. and Costantino Manes. Velocity measurements of a free-surface turbulent flow penetrating a porous medium composed of uniform-size spheres. Transport in porous media, 2009:**78**:367-383
[16] Vichnevetskey, R. B. Peiffer**.** Error waves in finite element and finite difference methods for hyperbolic equations. Advances in Computer Methods for Partial Differential Equations, AICA, Ghent, Belgium; 1975:53–58.
[17] Higashino, M. and Stefan, H**.** Velocity pulse model for turbulent diffusion form flowing water into a sediment bed". Journal of environmental engineering, 2008:**134**:550-560.
[18] Shavit, U., G. Bar-Yosef, R. Rosenzweig, and S. Assouline. Modified Brinkman equation for a free flow problem at the interface of porous surfaces: The Cantor-Taylor brush configuration case. Water resources research, 2002:**38**:56-1-56-13.
[19] Scheidegger, A. E. The physics of flow through porous media. New York: MacMillan; 1960.
[20] Schneebeli, G. Hydraulique souterraine. Paris: Eyrolles Editeurs, 1966.
[21] Baver, L. D., Gardner, W. H., Gardner, W. R. *Soil physics (4th ed.)*. New York: Wiley; 1972.
[22] DePinto, J. V., Lick, W., and Paul, J. Transport and transformation of contaminants near the sediment-water interface, CRC, Boca Raton, Fla, 1994.
[23] Bear, J. *Dynamics of fluids in porous media*. New York: American Elsevier; 1972.
[24] Boudreau, B. P. A mathematical model for sediment-suspended particle exchange. J. Mar. Syst, 1997:**11**:279–303.
[25] Karniadakis GE, Israeli M, and Orszag SA. High-order splitting methods for the incompressible Navier-Stokes equations. Journal of Computational Physics, 1991:**97**:414–443.
[26] Peyret R. Spectral Methods for Incompressible Viscous Flow. Springer-Verlag, 2002:**142**:434.
[27] Diamessis PJ, Domaradzki JA. and Hesthaven JS. A spectral multidomain penalty method model for the simulation of high Reynolds number localized stratified turbulence. Journal of Computational Physics, 2005:**202**:298–322.
[28] Hesthaven JS. A. Stable penalty method for the compressible Navier-Stokes equations: III. multidimensional domain decomposition schemes. SIAM Journal of Scientific Computing, 1998:**20:**62–93.
[29] Escobar-Vargas J. A., Diamessis P. J. and Sakai T. A. Spectral quadrilateral multidomain penalty method model for high Reynolds number incompressible stratified flows. International Journal for Numerical Methods in Fluids, 2014:**75**:403-425.
[30] Hesthaven JS. A. Stable penalty method for the compressible Navier-Stokes equations: II. one-dimensional domain decomposition schemes. SIAM Journal of Scientific Computing, 1997:**18**:658–685.
[31] Hesthaven JS. and Gottlieb D. A. Stable penalty method for the compressible Navier-Stokes equations: I. open boundary conditions. *SIAM Journal of Scientific Computing*; 1996:**17**:579–612.
[32] Blackburn HM. and Schmidt S. Spectral element filtering techniques for large eddy simulation with dynamic estimation. Journal of Computational Physics, 2003:**186**:610–629.
[33] Escobar-Vargas JA. A spectral multidomain penalty method solver for environmental flow processes. Ph.D. Thesis, Cornell University, 2012.